Title: Multi-omic analysis of HDAC1 function in pancreatic cancer reveals altered GTPase activity impacting chemoresistance

Authors: Carter A. Wright[1,2], Emily R. Gordon[2], Sara J. Cooper[2]

Affiliations:
[1]The University of Alabama in Huntsville, Huntsville, AL
[2]HudsonAlpha Institute for Biotechnology, Huntsville, AL

Corresponding author: Sara J. Cooper, sjcooper@hudsonalpha.org
ORCID: 0000-0002-9627-0309

Abstract

Background

Multi-drug resistance is a key factor controlling patient outcomes in pancreatic ductal adenocarcinoma (PDAC). A mechanistic understanding of resistance enables development of novel treatments and precision medicine. Chromatin remodeling, mediated by altered expression and function of regulators including HDAC1, is one mechanism of resistance. We describe a multi-omic analysis of *HDAC1*, a histone deacetylase involved in several chromatin remodeling complexes, to understand how overexpression contributes to multi-drug resistance and patient survival in PDAC.

Methods

We overexpressed *HDAC1* in MIA PaCa-2 cells using CRISPRa and characterized gene expression and HDAC1 function using RNA-sequencing and ChIP-sequencing for HDAC1 and H3K27 acetylation. Analysis of HDAC1 targets revealed altered GTPase activity, which was confirmed using a biochemical assay.

Results

HDAC1 overexpression in PDAC facilitates multi-drug resistance by promoting a stem-like state through global chromatin remodeling. A downstream result is increased GTPase activity which can be reversed by chemical inhibition or knockdown of HDAC1. HDAC1 target genes identified using *in vitro* and *in vivo* analysis led to the development of a clinically relevant nine-transcript prognostic signature that predicts patient prognosis.

Conclusions

Integrative genomic analysis demonstrates HDAC1's role in promoting drug resistance. These findings fuel the advancement of novel strategies for treatment and precision oncology.

Background

Pancreatic ductal adenocarcinoma (PDAC) is the most common form of pancreatic cancer and one of the most lethal cancers with a five-year survival rate of 11.5%. Due to the lack of early-stage symptoms, 52% of patients are diagnosed with unresectable, locally advanced, metastatic cancer[1]. Chemotherapeutics such as gemcitabine, abraxane, and combination therapies like FOLFIRINOX are standard of care treatments to improve prognosis, but chemoresistance develops in the majority of patients and contributes to the poor outcomes.

PDAC tumor cells achieve drug resistance through many cellular mechanisms. For example, over-activation of DNA damage repair processes limits the effectiveness of nucleoside analogs like gemcitabine. Tumors acquiring a mesenchymal phenotype, activated through genes involved in the epithelial to mesenchymal transition (EMT), become more invasive and have increased migratory

potential[2]. Additionally, the hypovascular nature of PDAC tumors prevents sufficient delivery of oxygen to the tumor cells. This hypoxic environment promotes overexpression of anti-apoptotic genes (i.e. *Bcl-XL* and *FLIP*), suppressing apoptosis and contributing to drug resistance[2,3,4,]. Reduced blood flow also restricts delivery of drugs to tumors, further exacerbating resistance. Understanding mechanisms of drug resistance can facilitate development of therapeutic strategies to prevent or reverse resistance.

Previous work, including our own publications, linked chromatin remodeling genes to chemoresistance and patient survival in PDAC[5–7]. Chromatin remodeling is a mechanism of gene regulation through rearrangement of chromatin structure to alter DNA accessibility and influence transcription factor binding. This process can alter gene expression patterns and lead to cellular reprogramming that contributes to chemoresistance. Dysregulation of chromatin remodeling genes leads to global changes in gene expression making it difficult to determine whether chromatin remodeling alters known resistance pathways, novel resistance pathways, or a combination[8].

We previously demonstrated that overexpression of *HDAC1* contributes to multidrug resistance in pancreatic cancer cells[9]. While HDACs are canonically members of repressive complexes, binding of HDAC1 has also been associated with transcriptional activation. In some cases, this is explained by HDAC1's ability to recruit RNA Pol II or regulate transcriptional elongation[10,11]. HDAC1 participates in several remodeling complexes including Sin3A, NuRD, and CoREST[12]. In cancer, HDAC1 regulates the acetylation of histone and non-histone proteins which modulate the expression of genes that influence cancer progression[8]. For example, the Sin3A complex, including HDAC1 is recruited to the promoter of *CDH1*, an epithelial cell marker, where it silences *CDH1* expression during metastasis[8]. HDAC1 regulates expression of several genes involved in resistance pathways including apoptosis, DNA damage repair, metastasis, and EMT[8,13].

The ability of HDAC1 to regulate genes is important for drug resistance, cancer progression, and tumor suppression making it a strong candidate as a drug target. Several HDAC inhibitors (HDACi) have been tested (e.g. entinostat, romidepsin) for the treatment of solid tumors and hematological malignancies[14]. However, clinical trials for HDACis in PDAC have been largely unsuccessful[14,15]. HDAC inhibition by commercially available HDACis leads to negative side effects in patients[16] since HDACs have a broad impact on expression of genes involved in cancer pathways and normal cellular functions including the function of non-histone proteins; thus, inhibition of multiple HDACs using molecules that target a class of proteins causes global effects. Using genomic analyses of an *in vitro* system perturbing HDAC1 function, we identify genes and pathways which are regulated by HDAC1 and contribute to chemoresistance. These genes represent future targets for drug development and potential markers of treatment response in patients with elevated *HDAC1* expression.

In this study, we overexpressed *HDAC1* in a well described PDAC cell line, MIA PaCa-2, and measured the effects on gene expression, HDAC1 binding, and chromatin structure to better understand how HDAC1 activation contributes to resistance. We found that HDAC1 overexpression leads to altered activity of pathways (e.g. EMT, resistance to apoptosis, altered cell cycle checkpoint, and increased hypoxia) that each have the potential to contribute to resistance. We showed that *HDAC1* overexpression leads to a more mesenchymal phenotype *in vitro* and observed that *HDAC1* overexpression in patient tissues alters these pathways in a similar way. Using ChIP-seq, we determined that the genes bound and regulated by HDAC1 were enriched for GTPases and expression of these genes in patient tissues were negatively correlated with patient survival. We showed that *HDAC1* overexpression results in altered expression of GTPases and thus increased GTPase activity suggesting that altered GTPase activity contributes to chemoresistance and represents possible targets to reverse resistance. Together these data reveal an improved mechanistic understanding of the role of HDAC1 in chemoresistance and nominate GTPase genes as potential therapeutic targets.

Results

HDAC1 overexpression leads to multi-drug resistance

HDAC1 expression has been previously linked to increased cellular resistance to cytotoxic chemotherapeutic drugs[9]. To further evaluate the effects of *HDAC1* overexpression on chemotherapeutic resistance, we used CRISPRa[17] to generate a stable MIA PaCa-2 cell line (MP2_HDAC1_OE) expressing *HDAC1* at ~3 times the levels of the levels of the control line (MP2_NTC) which expresses a non-targeting control guide (**Supplementary Data Fig. 1a**). We also treated the MIA PaCa-2 cell line with a HDAC1 siRNA to evaluate the effects of reducing *HDAC1* expression on chemoresistance (MP2_HDAC1_KD). MIA PaCa-2 is a well-characterized line with modest to high expression of *HDAC1*[18]. *HDAC1* is the most abundantly expressed HDAC gene in this line (**Supplementary Fig. 1b**). Under these three conditions, we measured the effect of treatment with irinotecan, gemcitabine, and oxaliplatin on cell viability (**Fig. 1a-c**). MP2_HDAC1_OE cells were more resistant to drug treatment than control cells and MP2_HDAC1_KD cells. Since *HDAC1* overexpression led to increased resistance to these drugs, we evaluated the effect of HDAC1 protein inhibition on drug response. We treated MP2_HDAC1_OE and MP2_NTC lines with romidepsin, a HDAC1/2 inhibitor, in combination with increasing concentrations of irinotecan. We observed a sensitizing effect of romidepsin on the MP2_HDAC1_OE cells treated with irinotecan (**Fig. 1d**). Together these experiments show a sensitizing effect of decreasing HDAC1 activity through either chemical inhibition or decreased expression.

HDAC1 overexpression induces expression of markers of EMT *in vitro* and in human PDAC tissues

We performed RNA-sequencing to measure gene expression in MP2_HDAC1_OE and MP2_NTC cells. We found 1,259 genes that are differentially expressed with overexpression of *HDAC1* (padj < 0.1). These differentially expressed genes (DEG) were enriched for pathways involved in drug resistance: apoptosis, EMT, G2-M checkpoint, and hypoxia (**Fig. 2a, Supplementary Fig. 2**). Alteration of EMT-associated DEG promotes invasion and migration associated with a more drug resistant mesenchymal cell state[19]. The cell surface marker CD44 is characteristic of the mesenchymal phenotype[20,21]. We detected a 1.8-fold increase in *CD44* expression upon overexpression of *HDAC1*. Consistent with the expression data, immunohistochemistry showed a comparable 2-fold increase in relative density of CD44 protein in PDAC cell lines with *HDAC1* overexpression (**Fig. 2b,c**).

These data provide evidence that *HDAC1* overexpression modulates several known resistance pathways including induction of EMT in an *in vitro* model. Next, we sought to determine whether *HDAC1* overexpression in patient tumors leads to similar changes in gene expression. We used RNA-sequencing data collected from pancreatic tumor tissues by The Cancer Genome Atlas (TCGA-PDAC dataset). We grouped tissues based on their expression of *HDAC1*. We compared the lowest (n=45, $HDAC1^{HIGH}$) and highest (n=45, $HDAC1^{LOW}$) quartiles of *HDAC1* expressing samples to identify DEG in these tissues. We identified 10,592 DEG between $HDAC1^{HIGH}$ and $HDAC1^{LOW}$ tissues. We intersected this gene list with the 1,259 genes identified in our *in vitro* experiment and identified 322 genes that are significantly altered (padj < 0.1) in the same direction as we observed in cell lines. Heatmaps of the DEG in both datasets were clustered by sample which separated high and low *HDAC1* expression (**Fig. 3a,b**). This analysis indicates that there is a similar pattern of expression in the PDAC tissues with high HDAC1 expression as in the MP2_HDAC1_OE cells.

Given our previous finding that *HDAC1* overexpression can lead to *in vitro* drug resistance we wondered whether *HDAC1* expression might be associated with patient response to treatment. In the TCGA dataset, we used patient prognosis information, specifically overall survival, as a proxy for treatment response. We hypothesized that given HDAC1's role in cellular resistance, genes associated with *HDAC1* overexpression might have prognostic value. We divided the 322 genes associated with increased *HDAC1* expression in both patient tissues and in the MP2_HDAC1_OE line into two groups: upregulated genes (n = 216) and downregulated (n = 106) genes. For each gene set, we calculated a mean gene expression value from TCGA PDAC patient tissues and compared the top and bottom quartiles in a survival analysis. We determined that overall survival was shortened for patients with high expression of the upregulated genes and low expression of the downregulated genes (upregulated genes p = 0.00065, downregulated genes p = 0.0051, **Fig. 3c,d**). Although overall survival depends on multiple factors, including treatment response, this finding is consistent with our observation that *HDAC1* overexpression is associated with drug

resistance *in vitro* and supports the hypothesis that these genes might also impact drug response in patients and lead to decreased survival time. Importantly, overexpression of *HDAC1* alone is not predictive of patient survival (p=0.44**, Supplementary Fig. 3**). Using an independent cohort (Kirby et al. 2016), we observed a similar difference in survival based on HDAC1-regulated genes (**Supplementary Fig. 4a,b**, upregulated genes p = 0.064, downregulated genes p = 0.19).

We wanted to determine whether combining the data we generated from cell lines with patient tumor data improved survival predictions. We compared prognostic predictions from the 322 DEG associated with HDAC1 expression in both TCGA PDAC tumors and HDAC1_OE cell lines in **Figure 3** with the top 322 DEG in TCGA PDAC samples with high and low *HDAC1* expression as well as the top 322 DEG in our PDAC cell lines with *HDAC1* overexpression and controls. We observe a more significant p-value for overall survival when combining our *in vitro* data with patient data than when using DEG from cell lines or TCGA PDAC tumors individually (**Supplementary Fig. 5a-d**).

Gene set enrichment analysis of the 322 DEG revealed multiple cancer processes including cadherin binding, cell-cell adhesion, regulation of cell migration, and GTPase activity (**Fig. 3e**, **Supplementary Table 1**). Some of these are well described resistance pathways, but GTPase activity has not been thoroughly explored for its role in resistance. Among the enriched GTPase genes is *RAP2B,* which was upregulated upon *HDAC1* overexpression (**Supplementary Fig. 6a,b**). When activated, this GTP-binding protein promotes cell migration, cell adhesion, proliferation, and metastasis in cancer[22–24].

HDAC1 overexpression alters chromatin accessibility in distal enhancer and promoter regions nearby molecular switches

To identify direct and indirect impacts of *HDAC1* overexpression that might contribute to resistance, we measured genome-wide DNA binding of the HDAC1 protein and the presence of the activating histone mark, H3K27 acetylation (H3K27ac) using ChIP-sequencing in the MP2_HDAC1_OE and MP2_NTC cell lines. Using the standard ENCODE ChIP-seq protocol for peak calling[25], we identified 17,457 binding sites for HDAC1 (10,033 unique to MP2_HDAC1_OE, 3,789 unique to MP2_NTC). We found 30,961 regions of H3K27ac; 8,392 were unique to MP2_HDAC1_OE and 5,916 were unique to MP2_NTC (**Fig. 4a**). We observed an enrichment of HDAC1 binding and regions of H3K27ac near the transcription start sites (TSS) of DEG when *HDAC1* is overexpressed. The H3K27ac peaks specific to *HDAC1* overexpressing cells occurred significantly more near the upregulated genes despite HDAC1's canonical role as a repressor (**Supplementary Fig. 7,** p<0.1).

To identify regions with altered HDAC1 binding or H3K27 acetylation directly impacting gene expression, we overlapped 1kb regions centered on all HDAC1 and H3K27ac peaks (overlapping

peaks were merged, see Methods) with promoter regions of DEG (2kb upstream of annotated TSS). This revealed 1,857 regions of HDAC1 binding or H3K27 acetylation in promoters of 1,040 DEG (one promoter can have more than one overlapping peak). Gene set enrichment analysis of these 1,040 DEG revealed enrichment for GTPase activity, cadherin binding, and DNA binding (FDR < 0.05) (**Supplementary Table 2**).

To better understand how *HDAC1* overexpression impacts H3K27ac and influences gene expression, we divided regions of HDAC1 binding and H3K27 acetylation based on whether they were increasing or decreasing across the regions described above (500bp up and downstream centered on the peak). Using the sequencing reads collected in a region called as a peak in any of our ChIP-seq experiments, we calculated a fold-change to determine whether there was evidence of increased or decreased binding. Given HDAC1's canonical role as a repressor, we expected that increased HDAC1 binding would be associated with decreased H3K27 acetylation, however, we only identified 235 DEG with increased HDAC1 binding and reduced H3K27 acetylation in the promoter regions (+/- 2kb from TSS). In contrast, the promoters of 597 DEG had increased HDAC1 binding and increased H3K27 acetylation (fold-change > 1) upon *HDAC1* overexpression (**Supplementary Table 3**). Since previous studies have shown that HDAC1 binding can be found near active genes[10], we tested whether expression of DEG where we also measured changes in altered HDAC1 binding and H3K27 acetylation were associated with overall patient survival. We performed survival analysis comparing outcomes of patients with the top 25% and bottom 25% mean tumor gene expression of these 597 genes. Patients with the highest mean expression of upregulated genes and lowest mean expression of downregulated genes have worse overall survival (upregulated: p = 0.0021, **Fig. 4b,** downregulated: p = 0.023, **Supplementary Fig. 8a**). We also showed that *HDAC1* expression is significantly higher in patients with the top 25% of mean tumor gene expression of the 597 genes (**Supplementary Fig. 8b**).

A nine-gene signature of HDAC1 regulated genes predicts PDAC patient survival

Identification of prognostic signatures in PDAC could be of clinical utility. The analyses above identified 597 genes regulated by HDAC1 that predict patient outcomes using genes identified from *in vitro* and *in vivo* signatures of *HDAC1* overexpression, although expression of *HDAC1* alone is not prognostic. We calculated a simplified signature of patient prognosis using a multivariate logistic regression with L1 penalized log partial likelihood (LASSO) for feature selection[26]. From the 597 genes, LASSO identified a 9-transcript model sufficient to differentiate TCGA PDAC tumors with high and low *HDAC1* expression (**Supplementary Fig. 8c,d**). To determine the clinical relevance of the genes selected using the LASSO model, survival analysis was performed comparing the patients in the top and bottom quartile of predictor values from the regression and the group with the highest predictor values had worse overall survival (**Fig. 4c**, p = 0.037).

***HDAC1* overexpression leads to increased GTPase activity and chemoresistance**

The identification of many DEG upon *HDAC1* overexpression led us to explore pathways that have not been previously linked to chemoresistance. Pathway enrichment analysis of DEG with increased HDAC1 binding and H3K27 acetylation in promoters (n = 597) identified an enrichment for many known cancer pathways (**Supplementary Table 4**). Included on this list was Ras signaling, regulation of apoptotic signaling pathway, chromatin binding, and GTPase activity. GTPase activity was also significant in enrichment analyses described in **Figure 3** driven by overexpression of the GTPases and associated proteins (e.g. *RALB*, *RAB27B*, and *RAC1)* which have increased expression with *HDAC1* overexpression and are associated with worse overall patient survival (**Supplementary Fig. 9a**). ARHGAP5, a Rho family-GTPase activating protein (**Fig. 5a**), was also increased with *HDAC1* overexpression and we observed increased HDAC1 binding and H3K27 acetylation near its TSS (**Fig. 5b**). Since activation of GTPase activity is not a well described mechanism of drug resistance, we used RNA-sequencing data from 14 unmodified PDAC cells lines with varying response to gemcitabine (Data from Kirby 2016) to further support the hypothesis that GTPase activity alters cellular response to chemotherapy. We found that cell lines with increased expression of genes influencing GTPase activity had higher levels of resistance to gemcitabine (**Fig. 5c**). We identified a
total of 11 genes that modulate GTPase activity and they all show a similar pattern of increased expression in resistant cell lines (**Supplementary Fig. 9b).** Increased GTPase activity activates the MAPK and PI3K pathways which promote proliferation and survival in cancer[27]. KEGG[28] pathway mapping of these 597 DEG confirmed the increased expression of genes in the MAPK and PI3K pathways upon *HDAC1* overexpression (**Supplementary Fig. 10**).

Given the increased transcript levels of several GTPases (**Fig 5d**), we tested whether there was a measurable difference in GTPase activity upon HDAC1 overexpression. GTPase activity was measured through the detection of GTP remaining after a GTP hydrolysis reaction catalyzed by cell lysates from the MP2_HDAC1_OE line compared to the MP2_NTC line. MP2_HDAC1_OE cell lysates have significantly increased GTPase activity (**Fig. 5e**) compared to the MP2_NTC control line. Conversely, treatment of MP2_HDAC1_OE and MP2_NTC cells with romidepsin, a HDAC1/2 inhibitor, decreased GTPase activity ($p < 0.05$) (**Supplementary Table 5**). We also observed decreased GTPase activity in MP2_NTC cells with a siRNA targeting HDAC1 (MP2_NTC_siRNA_HDAC1) compared to MP2_NTC cells with a non-targeting siRNA (MP2_NTC_siRNA_Control). These data demonstrate that *HDAC1* overexpression increases GTPase activity and that inhibition of HDAC1 reverses the effect.

Methods

Cell Culture

MiaPaCa-2 cells (ATCC #CRM-CRL-1420) were cultured in D10 media: DMEM (Lonza #12-614Q) supplemented with 10% FBS (GELifeSciences #SH30071.03), and 0.5% penicillin-streptomycin (ThermoFisher #15140122). All cell lines were maintained at 37 °C and 5% CO2. Cells were cryopreserved with the addition of 10% DMSO (EMD #MX1458-6).

Plasmids

LentiCRISPRv2 (Addgene #52961) or lentiSAMv2 (Addgene #92062) and lenti-MS2-p65-HSF1-Hygro (Addgene #89308) were used to generate stable cell lines for gene knockout and activation, respectively. pMD2.G (Addgene #12259) and psPAX2 (Addgene #12260) were used to facilitate viral packaging of sgRNAs and single vector plasmids.

sgRNA Cloning

gRNA oligos were designed and cloned into their respective plasmids as described previously[17].

DsiRNA

IDT TriFECTa RNAi kit was used per manufacturer's protocol. 100,000 cells were seeded in 1 well of a 12 well tissue culture treated plate 24 hours prior to transfection. Cells were transfected using RNAiMax (ThermoFisher #13778-030) following manufacturer's recommended protocol. As indicated in the TriFecta kit (IDT #hs.Ri.HDAC1.13), TYE 563 transfection efficiency control, positive HPRT-S1 control, and negative (DS NC1) scrambled sequence control were utilized. Further assays were performed 48 hours after transfection. Expression was validated with each transfection with the IDT PrimeTime qPCR Assay system on an Agilent QuantStudio 6 Flex Real-Time PCR system.

DsiRNA Sequences:

IDT DsiRNA name	DsiRNA Sequence
hs.Ri.HDAC1.13.1-SEQ1	rArGrUrUrUrCrCrUrUrUrUrUrGrArGrArUrArCrUrArUrUTT
hs.Ri.HDAC1.13.1-SEQ2	rArArArArUrArGrUrArUrCrUrCrArArArArArGrGrArArArCrUrArG
hs.Ri.HDAC1.13.2-SEQ1	rCrUrGrGrArArCrUrGrCrUrArArArGrUrArUrCrArCrCrAGA
hs.Ri.HDAC1.13.2-SEQ2	rUrCrUrGrGrUrGrArUrArCrUrUrUrArGrCrArGrUrUrCrCrArGrGrA
hs.Ri.HDAC1.13.3-SEQ1	rArGrCrCrGrGrUrCrArUrGrUrCrCrArArArGrUrArArUrGGA
hs.Ri.HDAC1.13.3-SEQ2	rUrCrCrArUrUrArCrUrUrUrGrGrArCrArUrGrArCrCrGrGrCrUrUrG

qPCR Sequence IDs:

Gene	Exon	IDT primeTime Assay ID
HDAC1	1-2	Hs.PT.58.20534173
HDAC1	3-4	Hs.PT.58.38680914
ACTB	1-2	Hs.PT.39a.22214847
GAPDH	2-3	Hs.PT.39a.22214836
HPRT1	8-9	Hs.PT.58v.45621572

GTPase-Glo Assay Using Cell Lysates

In vitro GTPase activity was measured using the GTPase-Glo assay (Promega #V7681). We followed the protocol as described[29] with modifications for use of cell lysates. Cell lysates were made from the following cell lines: MP2_HDAC1_OE, MP2_NTC, MP2_NTC with siRNA targeting *HDAC1* (MP2_NTC_siRNA_HDAC1), MP2_NTC with a non-targeting siRNA (MP2_NTC_siRNA_Control), MP2_HDAC1_OE treated with 0.01 μM romidepsin, an HDAC1 inhibitor, and MP2_NTC treated with 0.01 μM romidepsin. Cells (2 x 10^6 per tube) were lysed in a lysis buffer containing 50 mM HEPES at pH 7.6, 150 mM NaCl, 10% Glycerol, 0.1% NP-40, and 2 mM $MgCl_2$. To generate the lysate, 10μL of lysis buffer per 100,000 cells was added to each cell pellet and resuspended. Lysates were mixed for 30 minutes at 4°C, vortexed in three 10 second intervals, then centrifuged at 4°C for 30 minutes at 16.1x RCF. A 2X GTP solution was prepared and the reaction was initiated following the manufacturer's protocol.

Modifications for cell lysates required background wells for each cell line. GTPase-Glo Buffer was added to cell lysates at a final concentration of 1 μL per 10,000 cells. After the GTPase reaction, 20μL was added to each respective background well. Luminescence was measured using a BioTek Synergy H5 plate reader. To calculate GTPase activity for each cell type, we calculated the difference between the luminescence of the experimental wells and background wells. GraphPad Prism 9 (version 9.3.1) was used for plotting bar charts and t-tests performed in GraphPad were unpaired, parametric, two-tailed with 95% confidence interval.

ChIP-sequencing

MP2_HDAC1_OE and MP2_NTC cells (2 x 10^7) were cross-linked, harvested, and DNA was precipitated using a commercial H3K27ac antibody (Abcam, ab4729). Libraries were constructed, pooled, and sequenced using an Illumina NovaSeq instrument with 75bp single-end reads. These

data were generated and analyzed using published ENCODE protocols (https://www.encodeproject.org/documents/).

Differential binding analysis was conducted using the “multiBigwigSummary" tool from the “deepTools" package[30]. Using this tool, a ChIP-seq score was generated for each sample and region using genomic coordinates defined as +/- 500 bp from the center of peaks defined using the published ENCODE protocol[25] and 1 kb upstream of all annotated genes. Regions were merged together if they overlapped. We omitted any regions with a ChIP-seq score less than 1 for both MP2_HDAC1_OE and MP2_HDAC1_NTC. Using the ChIP-seq score, we calculated a fold-change between MP2_HDAC1_OE and MP2_NTC for HDAC1 and H3K27ac in each defined region. The criteria for differentially bound regions was a fold-change greater than or less than one for HDAC1 binding and H3K27 acetylation.

3’ RNA-sequencing

Cell pellets were frozen at -80°C until RNA extraction. For RNA extraction 350 µl of RL Buffer plus 1% β-ME from the Norgen Total RNA extraction kit was added to each cell pellet and extraction proceeded per manufacturer’s instructions including use of the DNase kit (Norgen # 37500, 25720). RNA quality was verified with the Agilent BioAnalyzer RNA Nano 600 kit (cat# 5067-1512) with the RIN range between 9.2-10. RNA-sequencing libraries were made using Lexogen QuantSeq 3' mRNA-Seq Library Prep Kit FWD for Illumina kit (cat# 015.24) with 250 ng of RNA input. They were pooled and sequenced on an Illumina NextSeq 500 instrument with 75 bp single-end reads. Read counts averaged 4 million reads and an average Q30 of 91.28%. Lexogen’s BlueBee integrated QuantSeq data analysis pipeline was used for trimming, mapping, and alignment and the R package “DESeq2” was used for differential expression analysis.

Drug resistance screening

Cells were seeded in 96-well plates at 2000 cells/well. Seeded cells were dosed with a range of concentrations of each drug: gemcitabine (0-12.5nM), oxaliplatin (0-3.5uM), or irinotecan (0-5uM). Cells were given a second dose of drug at the same concentration as the first 48 hours later. The number of viable cells surviving drug treatment were assayed with CellTiter-Glo (Promega #G7571) 24 hours after the last drug treatment per manufacturer's protocol using a BioTek Synergy H5 plate reader.

HDAC1 inhibition with romidepsin (Sigma #SML1175-1MG) was performed similarly to above except that cells were dosed every 24 hours with either 0.01 µM romidepsin, a range of gemcitabine, or both. Equal volume DMSO was used as a control in place of romidepsin. The number of viable cells surviving drug treatments were assayed with CellTiter-Glo (Promega #G7571) 24 hours after the last drug treatment per manufacturer's protocol using a BioTek Synergy

H5 plate reader. In both cases, data were plotted using GraphPad Prism 9, version 9.3.1. T-tests performed were unpaired, parametric, two-tailed with 95% confidence interval.

Cell staining

75,000 MIA PaCa-2 cells with non-targeting, HDAC1 OE sgRNAs, or HDAC1 KD with DsiRNA were seeded in 12 well plates. Cells were stained using Alexa Fluor 488 Conjugate kit for live cell imaging (LifeTechnologies #A25618) for CD44 via the manufacturer's protocol. DAPI (Invitrogen #D21490) was counterstained per manufacturer's protocols for adherent cells. Presence of CD44 in the cells was quantified using ImageJ 1.53K with measurements (area, mean, and integrated density) for stain and background taken with the freehand selection tool. Relative CD44 intensity or bound CD44 per area was calculated for each cell by: integrated density of cell-integrated density of background for that cell/area of that cell. GraphPad Prism 9 (version 9.3.1) was used for plotting violin plots and t-tests performed in GraphPad were unpaired, parametric, two-tailed with 95% confidence interval.

Enrichment Analysis

Enrichr, a comprehensive gene set analysis web server, and the R package "ClusterProfiler" (version 3.12.0)[31] were used for enrichment analysis of the differentially expressed genes[32]. We focused on the pathways (MSigDB) and gene ontology terms (GO MF, GO BP) reaching the significance threshold of FDR < 0.05.

Survival Analysis

To conduct survival analysis, clinical and RNAseq expression data was retrieved from The Cancer Genome Atlas (TCGA) for 178 PDAC (TCGA-PAAD) patients (https://portal.gdc.cancer.gov/). Data was normalized using the R package "DESeq2"[33] and differentially expressed genes with an FDR < 0.1 were used to generate Kaplan-Meier survival curves. We classified tissues based on their mean expression of a given gene set (bottom, middle, and top quartiles of gene expression). We compared the patients with the lowest and highest quartile of mean gene expression and performed survival analysis. Survival curves and analyses were generated using the "ggplot2", "survminer", and "survival" R packages[34–36].

Clinical Data and Samples

Clinical data and RNA-sequencing data for TCGA PDAC samples were retrieved on 04/01/2020 using the GDC Data Portal. Our analyses included 178 samples in this cohort that had matched clinical and RNA-sequencing data.

Data Access

ChIP-sequencing data is available using the GEO accessions GSE209895 (H3K27ac) and GSE158541 (HDAC1). RNA-sequencing is available using the GEO accessions GSE79668 and GSE79669 (gemcitabine resistant and sensitive cell lines)[37].

Statistical Testing

Statistical analysis was conducted in R (version 1.2.1335). The following R packages and software were used for analysis:

survival (version 1.2.1335)[35]

survminer (version 0.4.9)[36]

ggplot2 (version 3.3.6)[34]

DESeq2 (version 1.24.0)[33]

pheatmap (version 1.0.12)[38]

clusterProfiler (version 3.12.0)[31]

glmnet (version 4.1-3)[39]

ROCR (version 1.0-11)[40]

deepTools (version 3.5.0)[30]

IGV (version 2.7.2)[41]

LASSO model selection

A predictive gene signature from transcripts that are differentially expressed (DESeq2 FDR < 0.1) and have increased HDAC1 binding and H3K27 acetylation near their TSS (+/- 2000 bp) was developed using the LASSO regression model. LASSO was performed using the R package "glmnet" (version 4.1-3)[39]. The TCGA PDAC cohort was split into three groups by *HDAC1* expression (top 25%, middle 50%, and bottom 25%). The cohort was further subset by randomly distributing an equal number of samples from the top 25% and bottom 25% of *HDAC1* expression into two groups (n = 45). The training cohort and the validation cohort used the same dichotomization threshold (top 25% and bottom 25% of *HDAC1* expression). Model performance was evaluated based on the model's ability to classify patients into the high or low *HDAC1* expression group. We generated an area under the curve (AUC) value using the R package "ROCR" (version 1.0-11)[40]. Kaplan-Meier curves were generated using the R package "survival" (version 3.2-13)[35].

Data Analysis

The adjusted p-value was used to determine the top 322 differentially expressed genes in TCGA PDAC samples for comparison of patients in the top and bottom quartile of *HDAC1* expression. Using the R package "DESeq2" (version 1.24.0)[33], differentially expressed genes were excluded from the analysis if baseMean < 10.

Discussion

Pancreatic cancer ranks among the deadliest cancers due to its chemoresistant nature and insufficient treatment options. Understanding what drives chemoresistance is essential to identifying new therapeutic targets and improving patient outcomes. Chromatin remodeling has been established as a critical feature of tumorigenesis and cancer progression, making the pathway an attractive drug target. Our work and others showing the importance of key genes like *HDAC1* in chemoresistance have nominated chromatin remodeling genes as possible drug targets. Using genomic and biochemical approaches we revealed potential mechanisms by which *HDAC1* OE contributes to chemoresistance and showed that HDAC1 inhibition sensitizes PDAC cells to chemotherapeutic treatment further strengthening the argument that this pathway is a good candidate for treatment, however HDAC inhibitors have faced challenges in clinical trials. Commercial HDAC inhibitors target a class of HDACs and not specific proteins. This cross-reactivity leads to genome-wide off target effects and patient toxicity. That has motivated the current study which aims to better understand how *HDAC1* activation contributes to resistance and reveal novel downstream targets that may lead to alternative treatment strategies.

In contrast to other tumor types, multiple large scale drug trials that used targeted therapy were not as successful in pancreatic cancer[42,43], thus using a targeted gene panel that can be used to better define potential treatment options for PDAC patients could lead to improved survival and quality of life[44,45]. In this study, we collected data from an *in vitro* system testing the impact of *HDAC1* overexpression on PDAC cells and combined these results with information from publicly available gene expression data gathered from both tissues of PDAC patients and PDAC cell lines to show that *HDAC1* overexpression regulates a set of transcriptomic responses that contribute to chemoresistance and the genes regulated by HDAC1 can also be shown to predict patient outcome. *HDAC1* overexpression alone is not significantly prognostic of worse overall survival in PDAC patients. However, the genes altered by *HDAC1* overexpression are prognostic. Since HDAC1 is a genome-wide regulator of gene expression, in PDAC, we hypothesize that the genes contributing to a worse overall survival prognosis, resulting from tumorigenesis and drug resistance, are the subset of genes altered by *HDAC1* overexpression. These results show that pathways under the control of HDAC1 contribute to patient outcomes and could be used to predict outcomes that may be linked to treatment response. Of the 597 genes altered by *HDAC1* expression *in vitro*, we identified a 9-transcript novel signature that successfully predicted patients with high and low *HDAC1* expression and was correlated with patient survival. These analyses provided insight into a subset of genes that are regulated by HDAC1 and are predictive of worse patient survival, suggesting a potential clinical utility. Our panel of biomarkers represents a potential step forward in the development of an assay that is predictive of patient survival which could influence treatment decisions.

We integrated several datasets to better understand how *HDAC1* overexpression impacts PDAC cells. These studies revealed several processes known for their role in tumorigenesis, progression and drug resistance. One of these was EMT. In addition to its role in progression, EMT is associated with suppression of proteins involved in drug transport, such as CNT3, allowing the cells to evade the anti-proliferative effects of chemotherapeutics (gemcitabine)[46]. Cells that undergo EMT also have a more stem cell-like phenotype making them more resistant to chemotherapeutics[2]. Increased expression of *CD44*, a cell surface protein important for cell adhesion and migration, is associated with a more mesenchymal-like phenotype which is characteristic of EMT[20]. Here we have shown that the mesenchymal marker, CD44 transcript and protein are more abundant in cells with *HDAC1* overexpression, agreeing with our past work showing that *HDAC1* overexpression leads to increased migration[9].

Induction of EMT is also associated with drug resistance and we showed that MP2_HDAC1_OE cells are resistant to multiple drugs. Understanding the direct regulatory impacts of HDAC1 binding and H3K27ac occupancy is necessary to determine the impacts of *HDAC1* overexpression in pancreatic cancer. Our ChIP-seq experiments revealed altered H3K27 acetylation and HDAC1 binding near HDAC1 regulated genes. Interestingly, we found that the majority of the DEG with HDAC1 binding had an increase in HDAC1 and H3K27ac signals near their promoter. Our findings are in agreement with a previously published study concluding that HDAC1 binding is enriched at actively transcribed genes[10]. It is still not well understood how HDAC1 binding directly affects the activation of gene expression but Greer et al. did show that HDAC1 binding can regulate RNA Pol II recruitment and that HDAC1 may regulate transcription elongation through interaction with BRD4. Additionally, HDAC1 is known to deacetylate proteins other than histones which might facilitate activation of nearby transcription factors (e.g. MYC)[11].

Throughout this study, our gene set enrichment analyses of genes associated with *HDAC1* overexpression consistently revealed GTPase activity as an enriched process. A variety of proteins contribute to GTPase activity and many are druggable[47], which makes them of potential clinical interest. We have shown that expression of GTPases and GTPase activating proteins are associated with worse overall survival. We used biochemical assays to confirm that cells overexpressing HDAC1 have higher GTPase activity than control cells. This effect was reversible in cells treated with a HDACi, which reduced GTPase activity. GTPase signaling is important for pancreatic cancer initiation, metastasis, and invasion[48]. Increased GTPase signaling leads to the activation of key signaling cascades, such as MAPK and PI3K, that regulate cell proliferation, migration, and survival in cancer[27]. We have shown that the expression of genes in the MAPK and PI3K pathways are increased upon *HDAC*1 overexpression highlighting one known pathway altered by HDAC1 that contributes to PDAC progression[49]. GTPases, such as RAC1, have been shown to activate EMT pathway in multiple cancers, thus leading to a more invasive and drug resistant

phenotype[50–52] and we show that *RAC1* expression is increased upon *HDAC1* overexpression in PDAC cells. Additionally, ARHGAP5 is a GTPase activating protein associated with promoting EMT, a known mechanism of drug resistance in colorectal cancer, but its role in PDAC is not well understood[53]. We showed that expression of *ARHGAP5* and of several other proteins promoting GTPase activity are increased upon *HDAC1* overexpression and their transcripts are more abundant in gemcitabine resistant PDAC cell lines.

Despite decades of research, PDAC patients continue to have limited treatment options and suffer poor outcomes. Identifying patients who will benefit from existing treatments or those who need an alternative treatment is a key clinical need. Our work identified sets of genes that may help identify patients with poor prognosis due at least in part to treatment resistance and reveals novel therapeutic targets that may benefit patients experiencing resistance to treatment.

Additional Information:

Acknowledgements
We thank the Myers and Cooper labs for helpful feedback. We also acknowledge the data produced by The Cancer Genome Atlas which were extremely valuable and without which this study would not be possible. SJC is supported by UL1TR003096. SJC, ERG, and CAW are supported by Alabama's State Cancer Fund.

Authors' contributions
CAW, ERG, and SJC designed the experiments. CAW and ERG collected data. CAW and ERG analyzed the data. CAW and SJC wrote the first draft. All authors contributed to the writing of the paper and read and approved the final manuscript.

Ethics approval and consent to participate
Not applicable.

Data availability
ChIP-sequencing data is available using the GEO accessions GSE209895 (H3K27ac) and GSE158541 (HDAC1). RNA-sequencing is available using the GEO accessions GSE79668 and GSE79669.

Competing interests
None reported.

Funding information
This work was supported by Alabama's State Cancer Fund (to CAW, ERG, SJC). SJC received

support from the UAB CCTS grant (UL1TR003096).

References

1 Cancer of the pancreas - cancer stat facts. SEER. https://seer.cancer.gov/statfacts/html/pancreas.html (accessed 17 Oct2022).

2 Palamaris K, Felekouras E, Sakellariou S. Epithelial to Mesenchymal Transition: Key Regulator of Pancreatic Ductal Adenocarcinoma Progression and Chemoresistance. *Cancers* 2021; **13**. doi:10.3390/cancers13215532.

3 Shah VM, Sheppard BC, Sears RC, Alani AW. Hypoxia: Friend or Foe for drug delivery in Pancreatic Cancer. *Cancer Lett* 2020; **492**: 63–70.

4 Beatty GL, Werba G, Lyssiotis CA, Simeone DM. The biological underpinnings of therapeutic resistance in pancreatic cancer. *Genes Dev* 2021; **35**: 940–962.

5 Hasan N, Ahuja N. The Emerging Roles of ATP-Dependent Chromatin Remodeling Complexes in Pancreatic Cancer. *Cancers* 2019; **11**. doi:10.3390/cancers11121859.

6 Ying H, Dey P, Yao W, Kimmelman AC, Draetta GF, Maitra A *et al.* Genetics and biology of pancreatic ductal adenocarcinoma. *Genes Dev* 2016; **30**: 355–385.

7 McCleary-Wheeler AL, Lomberk GA, Weiss FU, Schneider G, Fabbri M, Poshusta TL *et al.* Insights into the epigenetic mechanisms controlling pancreatic carcinogenesis. *Cancer Lett* 2013; **328**: 212–221.

8 Li Y, Seto E. HDACs and HDAC Inhibitors in Cancer Development and Therapy. *Cold Spring Harb Perspect Med* 2016; **6**. doi:10.1101/cshperspect.a026831.

9 Ramaker RC, Hardigan AA, Gordon ER, Wright CA, Myers RM, Cooper SJ. Pooled CRISPR screening in pancreatic cancer cells implicates co-repressor complexes as a cause of multiple drug resistance via regulation of epithelial-to-mesenchymal transition. BMC Cancer. 2021; **21**. doi:10.1186/s12885-021-08388-1.

10 Wang Z, Zang C, Cui K, Schones DE, Barski A, Peng W *et al.* Genome-wide mapping of HATs and HDACs reveals distinct functions in active and inactive genes. *Cell* 2009; **138**: 1019–1031.

11 Greer CB, Tanaka Y, Kim YJ, Xie P, Zhang MQ, Park I-H *et al.* Histone Deacetylases Positively Regulate Transcription through the Elongation Machinery. *Cell Rep* 2015; **13**: 1444–1455.

12 Park S-Y, Kim J-S. A short guide to histone deacetylases including recent progress on class II enzymes. *Exp Mol Med* 2020; **52**: 204–212.

13 Hai R, He L, Shu G, Yin G. Characterization of Histone Deacetylase Mechanisms in Cancer Development. *Front Oncol* 2021; **11**: 700947.

14 Koutsounas I, Giaginis C, Theocharis S. Histone deacetylase inhibitors and pancreatic cancer: are there any promising clinical trials? *World J Gastroenterol* 2013; **19**: 1173–1181.

15 Hontecillas-Prieto L, Flores-Campos R, Silver A, de Álava E, Hajji N, García-Domínguez DJ. Synergistic Enhancement of Cancer Therapy Using HDAC Inhibitors: Opportunity for Clinical Trials. *Front Genet* 2020; **11**: 578011.

16 Laschanzky RS, Humphrey LE, Ma J, Smith LM, Enke TJ, Shukla SK *et al.* Selective Inhibition of Histone Deacetylases 1/2/6 in Combination with Gemcitabine: A Promising Combination for Pancreatic Cancer Therapy. *Cancers* 2019; **11**. doi:10.3390/cancers11091327.

17 Joung J, Konermann S, Gootenberg JS, Abudayyeh OO, Platt RJ, Brigham MD *et al.* Genome-scale CRISPR-Cas9 knockout and transcriptional activation screening. *Nat Protoc*

2017; **12**: 828–863.

18 Minami F, Sasaki N, Shichi Y, Gomi F, Michishita M, Ohkusu-Tsukada K *et al.* Morphofunctional analysis of human pancreatic cancer cell lines in 2- and 3-dimensional cultures. *Sci Rep* 2021; **11**: 6775.

19 Bulle A, Lim K-H. Beyond just a tight fortress: contribution of stroma to epithelial-mesenchymal transition in pancreatic cancer. *Signal Transduct Target Ther* 2020; **5**: 249.

20 Zhao S, Chen C, Chang K, Karnad A, Jagirdar J, Kumar AP *et al.* CD44 Expression Level and Isoform Contributes to Pancreatic Cancer Cell Plasticity, Invasiveness, and Response to Therapy. *Clin Cancer Res* 2016; **22**: 5592–5604.

21 Luu T. Epithelial-Mesenchymal Transition and Its Regulation Mechanisms in Pancreatic Cancer. *Front Oncol* 2021; **11**: 646399.

22 Li J, Song Y, Zhang C, Wang R, Hua L, Guo Y *et al.* TMEM43 promotes pancreatic cancer progression by stabilizing PRPF3 and regulating RAP2B/ERK axis. *Cell Mol Biol Lett* 2022; **27**: 24.

23 Miao F, Cui C, Zuo D, Zhang H, Mei P, Chen H *et al.* Rap2B promotes cell adhesion, proliferation, migration and invasion of human glioma. *J Neurooncol* 2019; **143**: 221–229.

24 Di J, Huang H, Qu D, Tang J, Cao W, Lu Z *et al.* Rap2B promotes proliferation, migration, and invasion of human breast cancer through calcium-related ERK1/2 signaling pathway. *Sci Rep* 2015; **5**: 12363.

25 Landt SG, Marinov GK, Kundaje A, Kheradpour P, Pauli F, Batzoglou S *et al.* ChIP-seq guidelines and practices of the ENCODE and modENCODE consortia. *Genome Res* 2012; **22**: 1813–1831.

26 Tibshirani R. Regression shrinkage and selection via the lasso. *J R Stat Soc* 1996; **58**: 267–288.

27 Soriano O, Alcón-Pérez M, Vicente-Manzanares M, Castellano E. The Crossroads between RAS and RHO Signaling Pathways in Cellular Transformation, Motility and Contraction. *Genes* 2021; **12**. doi:10.3390/genes12060819.

28 Kanehisa M, Furumichi M, Sato Y, Ishiguro-Watanabe M, Tanabe M. KEGG: integrating viruses and cellular organisms. *Nucleic Acids Res* 2021; **49**: D545–D551.

29 Mondal S, Hsiao K, Goueli SA. A Homogenous Bioluminescent System for Measuring GTPase, GTPase Activating Protein, and Guanine Nucleotide Exchange Factor Activities. *Assay Drug Dev Technol* 2015; **13**: 444–455.

30 Ramírez F, Dündar F, Diehl S, Grüning BA, Manke T. deepTools: a flexible platform for exploring deep-sequencing data. *Nucleic Acids Res* 2014; **42**: W187–91.

31 Yu G, Wang L-G, Han Y, He Q-Y. clusterProfiler: an R package for comparing biological themes among gene clusters. *OMICS* 2012; **16**: 284–287.

32 Chen EY, Tan CM, Kou Y, Duan Q, Wang Z, Meirelles GV *et al.* Enrichr: interactive and collaborative HTML5 gene list enrichment analysis tool. *BMC Bioinformatics* 2013; **14**: 128.

33 Love MI, Huber W, Anders S. Moderated estimation of fold change and dispersion for RNA-seq data with DESeq2. *Genome Biol* 2014; **15**: 550.

34 Wickham H. *ggplot2: Elegant Graphics for Data Analysis*. Springer International Publishing, 2016.

35 The survival package in R. Design of Experiments for Reliability Achievement. 2022; : 339–350.

36 Kassambara, Kosinski, Biecek, Fabian. survminer: Drawing Survival Curves using 'ggplot2'. *R package version 03*.

37 Kirby MK, Ramaker RC, Gertz J, Davis NS, Johnston BE, Oliver PG *et al.* RNA sequencing of pancreatic adenocarcinoma tumors yields novel expression patterns associated with long-term survival and reveals a role for ANGPTL4. *Mol Oncol* 2016; **10**: 1169–1182.

38 pheatmap: Pretty Heatmaps. Comprehensive R Archive Network (CRAN). https://cran.r-project.org/web/packages/pheatmap/index.html (accessed 9 Jul2022).

39 Hastie T, Qian J, Tay K. An Introduction to glmnet. *CRAN R Repositary* 2021.https://cloud.r-project.org/web/packages/glmnet/vignettes/glmnet.pdf.

40 Sing T, Sander O, Beerenwinkel N, Lengauer T. ROCR: visualizing classifier performance in R. *Bioinformatics* 2005; **21**: 3940–3941.

41 Thorvaldsdottir H, Robinson JT, Mesirov JP. Integrative Genomics Viewer (IGV): high-performance genomics data visualization and exploration. Briefings in Bioinformatics. 2013; **14**: 178–192.

42 Hecht JR, Lonardi S, Bendell J, Sim H-W, Macarulla T, Lopez CD *et al.* Randomized Phase III Study of FOLFOX Alone or With Pegilodecakin as Second-Line Therapy in Patients With Metastatic Pancreatic Cancer That Progressed After Gemcitabine (SEQUOIA). *J Clin Oncol* 2021; **39**: 1108–1118.

43 Tempero M, Oh D-Y, Tabernero J, Reni M, Van Cutsem E, Hendifar A *et al.* Ibrutinib in combination with nab-paclitaxel and gemcitabine for first-line treatment of patients with metastatic pancreatic adenocarcinoma: phase III RESOLVE study. *Ann Oncol* 2021; **32**: 600–608.

44 Hosein AN, Dougan SK, Aguirre AJ, Maitra A. Translational advances in pancreatic ductal adenocarcinoma therapy. *Nat Cancer* 2022; **3**: 272–286.

45 Wei X, Zhou X, Zhao Y, He Y, Weng Z, Xu C. A 14-gene gemcitabine resistance gene signature is significantly associated with the prognosis of pancreatic cancer patients. *Sci Rep* 2021; **11**: 6087.

46 Zheng X, Carstens JL, Kim J, Scheible M, Kaye J, Sugimoto H *et al.* Epithelial-to-mesenchymal transition is dispensable for metastasis but induces chemoresistance in pancreatic cancer. *Nature* 2015; **527**: 525–530.

47 Prieto-Dominguez N, Parnell C, Teng Y. Drugging the Small GTPase Pathways in Cancer Treatment: Promises and Challenges. *Cells* 2019; **8**. doi:10.3390/cells8030255.

48 Yoshimachi S, Shirakawa R, Cao M, Trinh DA, Gao P, Sakata N *et al.* Ral GTPase-activating protein regulates the malignancy of pancreatic ductal adenocarcinoma. *Cancer Sci* 2021; **112**: 3064–3073.

49 Mehra S, Deshpande N, Nagathihalli N. Targeting PI3K Pathway in Pancreatic Ductal Adenocarcinoma: Rationale and Progress. *Cancers* 2021; **13**. doi:10.3390/cancers13174434.

50 Fang D, Chen H, Zhu JY, Wang W, Teng Y, Ding H-F *et al.* Epithelial-mesenchymal transition of ovarian cancer cells is sustained by Rac1 through simultaneous activation of MEK1/2 and Src signaling pathways. *Oncogene* 2017; **36**: 1546–1558.

51 Zhou Y, Liao Q, Han Y, Chen J, Liu Z, Ling H *et al.* Rac1 overexpression is correlated with

epithelial mesenchymal transition and predicts poor prognosis in non-small cell lung cancer. *J Cancer* 2016; **7**: 2100–2109.

52 Ungefroren H, Witte D, Lehnert H. The role of small GTPases of the Rho/Rac family in TGF-β-induced EMT and cell motility in cancer. Developmental Dynamics. 2018; **247**: 451–461.

53 Tian T, Chen Z-H, Zheng Z, Liu Y, Zhao Q, Liu Y *et al.* Investigation of the role and mechanism of ARHGAP5-mediated colorectal cancer metastasis. *Theranostics* 2020; **10**: 5998–6010.

Fig 1. Quantification of cell viability in PDAC cell lines following treatment of chemotherapeutics
Quantification of viability following treatment with **a,** gemcitabine, **b,** oxaliplatin, and **c,** irinotecan in MP2_HDAC1_OE (blue triangles), MP2_NTC (pink squares), and MP2_HDAC1_KD (grey circles) cell lines. The bar represents the median. P-values were calculated using a two-tailed t-test. *p< 0.05, **p< 0.01, ***p<0.001, ****p<0.0005. ns, not significant. **d,** Quantification of cell viability following treatment with romidepsin, a HDAC1 inhibitor, in MP2_HDAC1_OE and MP2_NTC cell lines. Bar = median. P-values were calculated using a two-tailed t-test. *p< 0.05, **p< 0.01, ***p<0.001. ns, not significant.

Fig 2. *HDAC1* overexpression is associated with increased expression of EMT genes.
a, Expression of EMT genes in MP2_HDAC1_OE and MP2_NTC cell lines. Each column represents a replicate of the denoted cell line. The color scale denotes the z-score of each gene.
b, Brightfield images and immunofluorescent staining of DAPI (blue), CD44 (green), and merged CD44:DAPI (blue/green) of MP2_HDAC1_OE (bottom) and MP2_NTC (top) cells.
c, Violin plot analysis of immunofluorescent staining of CD44 in MP2_HDAC1_OE (blue) and MP2_NTC cells (pink). 100 cells were measured for each cell line. P-values were calculated using a two-tailed t-test. ****p<0.0001.

Fig 3. Genes altered by increased *HDAC1* expression in PDAC cell lines and TCGA PDAC samples are associated with patient survival.
a, Expression of DEG in MP2_HDAC1_OE (blue) and MP2_NTC (pink) cell lines. DEG are significantly (padj < 0.1) altered in the same direction in MP2_HDAC1_OE cells and TCGA PDAC tissues with the top 25% of *HDAC1* expression. Each column represents a replicate of the noted cell line. The color scale denotes the z-score of each gene.
b, Expression of DEG in TCGA PDAC samples. Each column represents a tumor sample. The color scale denotes the z-score of each gene. DEG are significantly (padj < 0.1) altered in the same direction in TCGA PDAC tissues with the top 25% of *HDAC1* expression and MP2_HDAC1_OE cells.
c, Overall survival of TCCA PDAC patients (n = 90) with top and bottom 25% of average gene expression of upregulated genes (n = 216) in **a** and **b**. P-values were derived using log-rank test.
d, Overall survival of TCCA PDAC patients (n = 90) with top and bottom 25% of average gene expression of downregulated genes (n = 106) in **a** and **b**. P-values were derived using log-rank test.
e, GO analysis showing enriched molecular functions using the genes (n = 322) in **a** and **b.**

Fig 4. ChIP-sequencing reveals DEG associated with patient survival
a, Venn diagram showing overlap of H3K27ac ChIP-seq peaks in MP2_HDAC1_OE and MP2_NTC cell lines.
b, Overall survival of TCCA PDAC patients (n = 90) with top (teal) and bottom (grey) 25% of average gene expression of upregulated DEG with increased HDAC1 binding and H3K27 acetylation in their promoter upon *HDAC1* overexpression. P-value was derived using log-rank test.
c, Overall survival of TCCA PDAC patients (n = 90) with top (blue) and bottom (red) 25% of predictor values generated from the nine-transcript LASSO model. P-value was derived using log-rank test.

Fig 5. *HDAC1* overexpression is associated with increased GTPase activity.
a, Normalized expression of *ARHGAP5* in MP2_HDAC1_OE (blue) and MP2_NTC (pink) cell lines. The bar is the median. P-values were calculated using an unpaired two-tailed t-test, p = 0.0003479.
b, ChIP-seq analysis of the ARHGAP5 promoter showing increased HDAC1 and H3K27ac peak

height in MP2_HDAC1_OE (blue) cells compared to MP2_NTC (pink) cells.
c, Normalized expression of *ARHGAP5* in PDAC cell lines resistant (blue) and sensitive (pink) to gemcitabine. The bar is the median. P-values were calculated using an unpaired two-tailed t-test, $p = 0.00831$.
d, Expression of DEG involved in GTPase activity in MP2_HDAC1_OE (blue) and MP2_NTC (pink) cell lines. Each column represents a replicate of the noted cell line. The color scale denotes the z-score of each gene.
e, Comparison of GTPase activity in the following cell lines: MP2_HDAC1_OE (blue), MP2_NTC (pink), MP2_NTC_siRNA_Control (grey), MP2_NTC_siRNA_HDAC1 (purple), MP2_HDAC1_OE and MP2_NTC treated with 0.1μM romidepsin (teal). P-values were calculated using a two-tailed t-test. **$p < 0.01$, **** $p < 0.0001$.

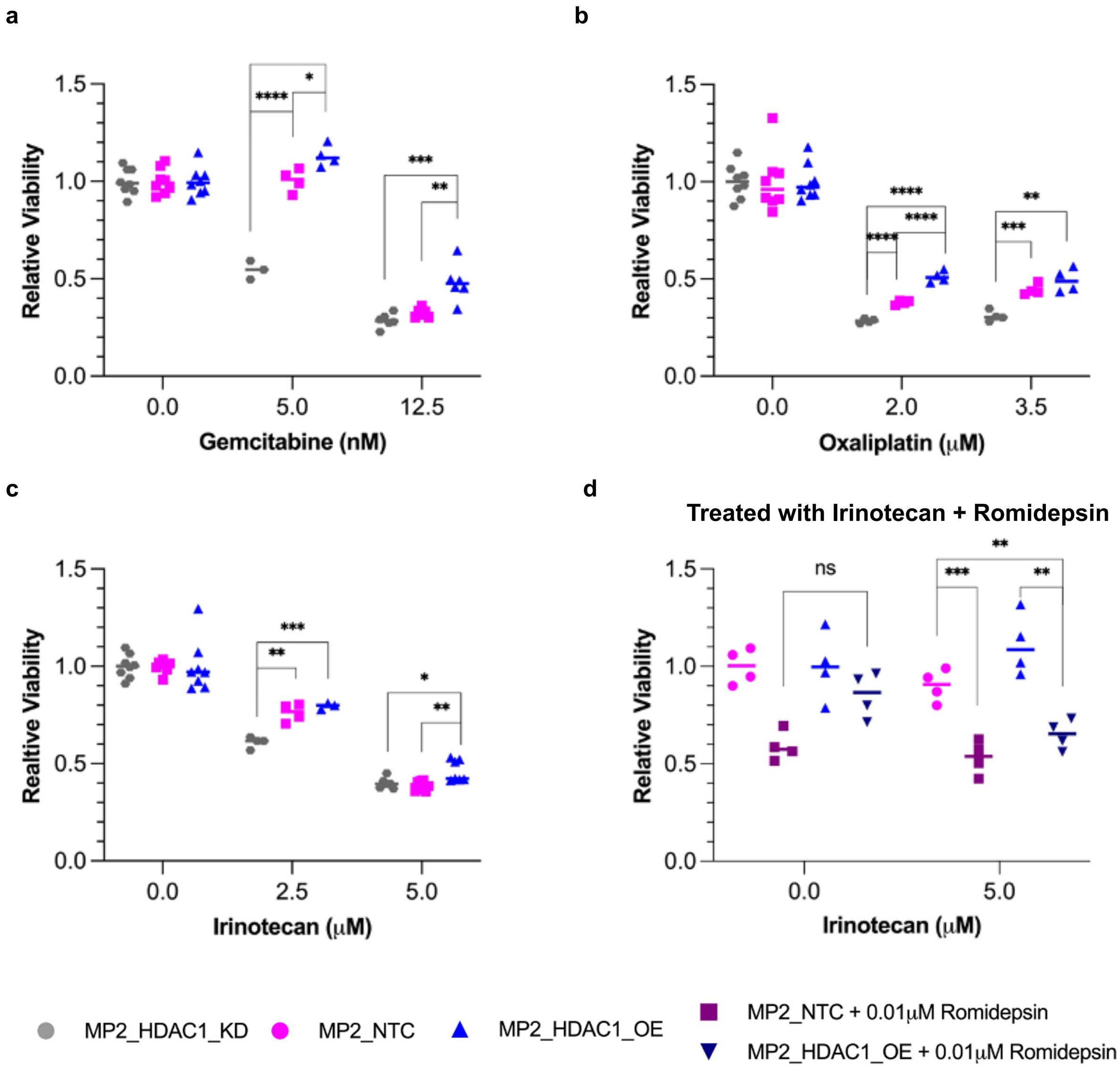
a
Relative Viability
1.5
1.0
0.5
0.0
****
*
***
**
0.0
5.0
12.5
Gemcitabine (nM)
b
Realtive Viability
1.5
1.0
0.5
0.0
****
****
****
**
***
0.0
2.0
3.5
Oxaliplatin (μM)
c
Realtive Viability
1.5
1.0
0.5
0.0
***
**
*
**
0.0
2.5
5.0
Irinotecan (μM)
d
Treated with Irinotecan + Romidepsin
Relative Viability
1.5
1.0
0.5
0.0
ns
**
***
**
0.0
5.0
Irinotecan (μM)
MP2_HDAC1_KD
MP2_NTC
MP2_HDAC1_OE
MP2_NTC + 0.01μM Romidepsin
MP2_HDAC1_OE + 0.01μM Romidepsin

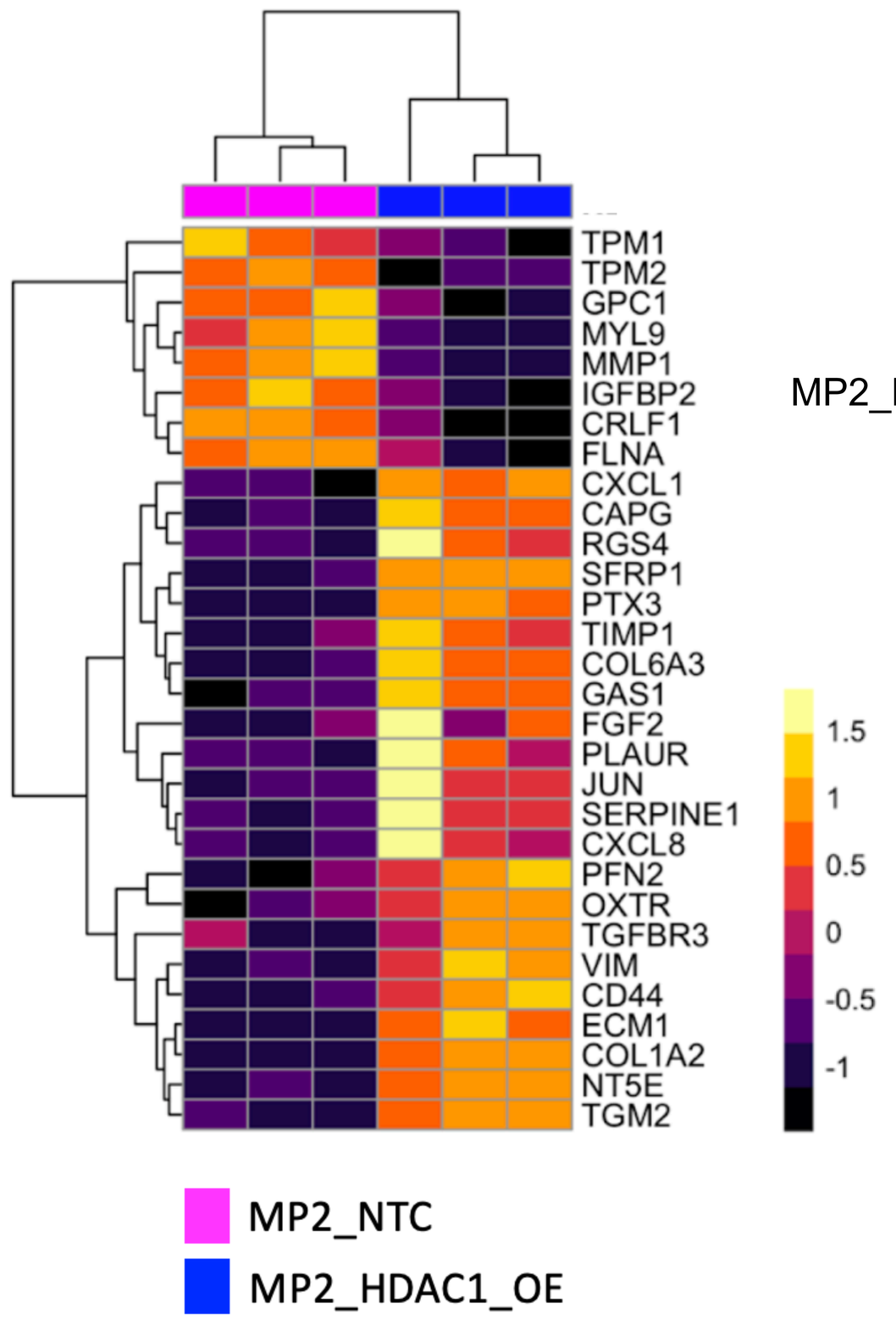
a
TPM1
TPM2
GPC1
MYL9
MMP1
IGFBP2
CRLF1
FLNA
CXCL1
CAPG
RGS4
SFRP1
PTX3
TIMP1
COL6A3
GAS1
FGF2
PLAUR
JUN
SERPINE1
CXCL8
PFN2
OXTR
TGFBR3
VIM
CD44
ECM1
COL1A2
NT5E
TGM2
1.5
1
0.5
0
-0.5
-1
MP2_NTC
MP2_HDAC1_OE

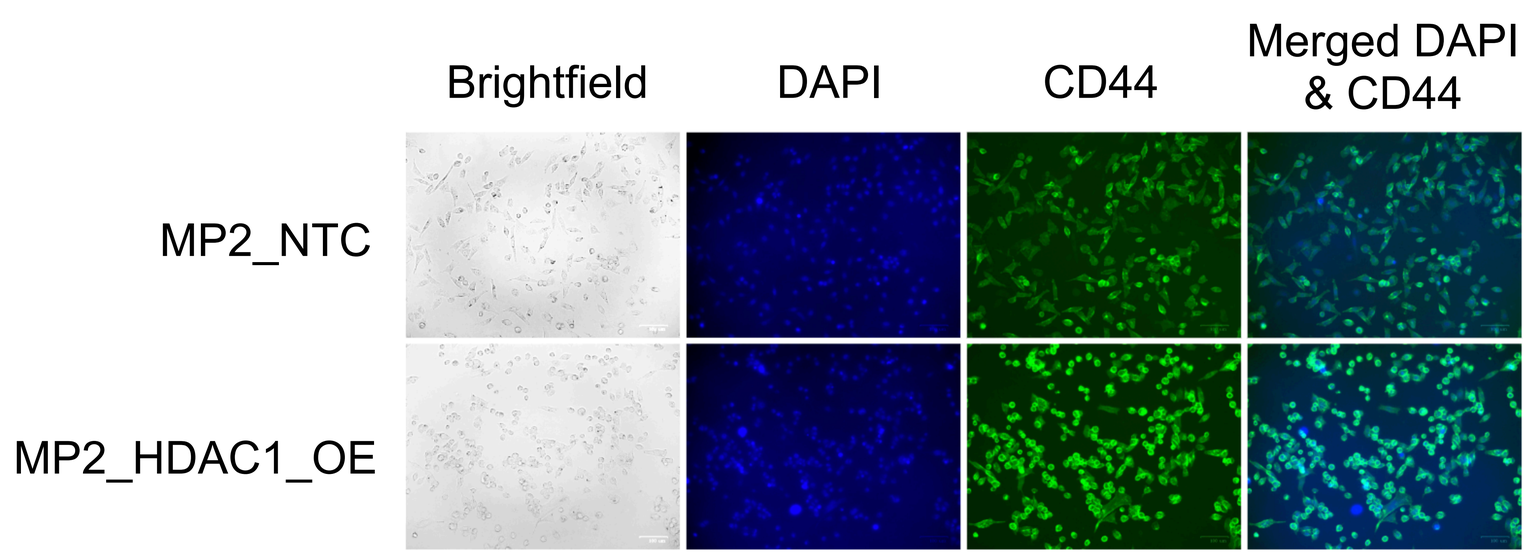
b
Brightfield
DAPI
CD44
Merged DAPI & CD44
MP2_NTC
MP2_HDAC1_OE

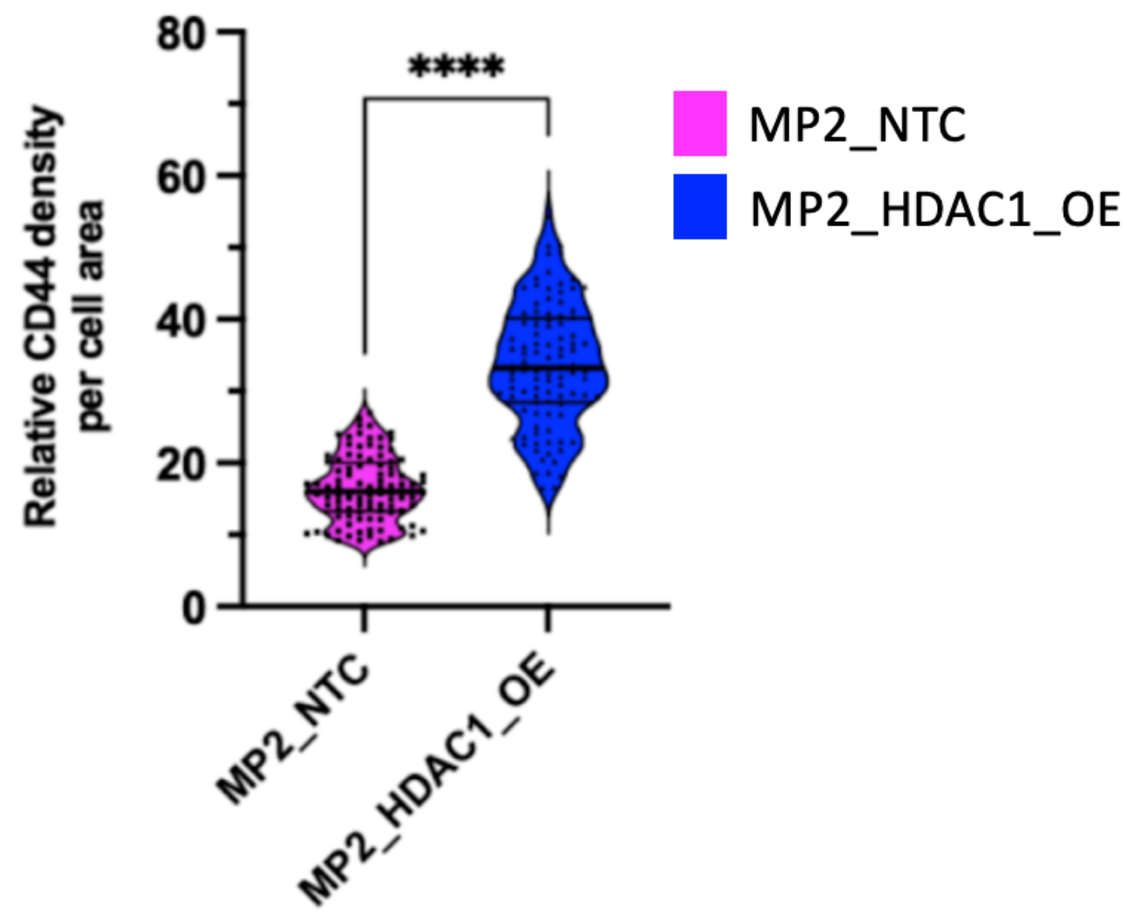
c
Relative CD44 density per cell area
80
60
40
20
0
****
MP2_NTC
MP2_HDAC1_OE
MP2_NTC
MP2_HDAC1_OE

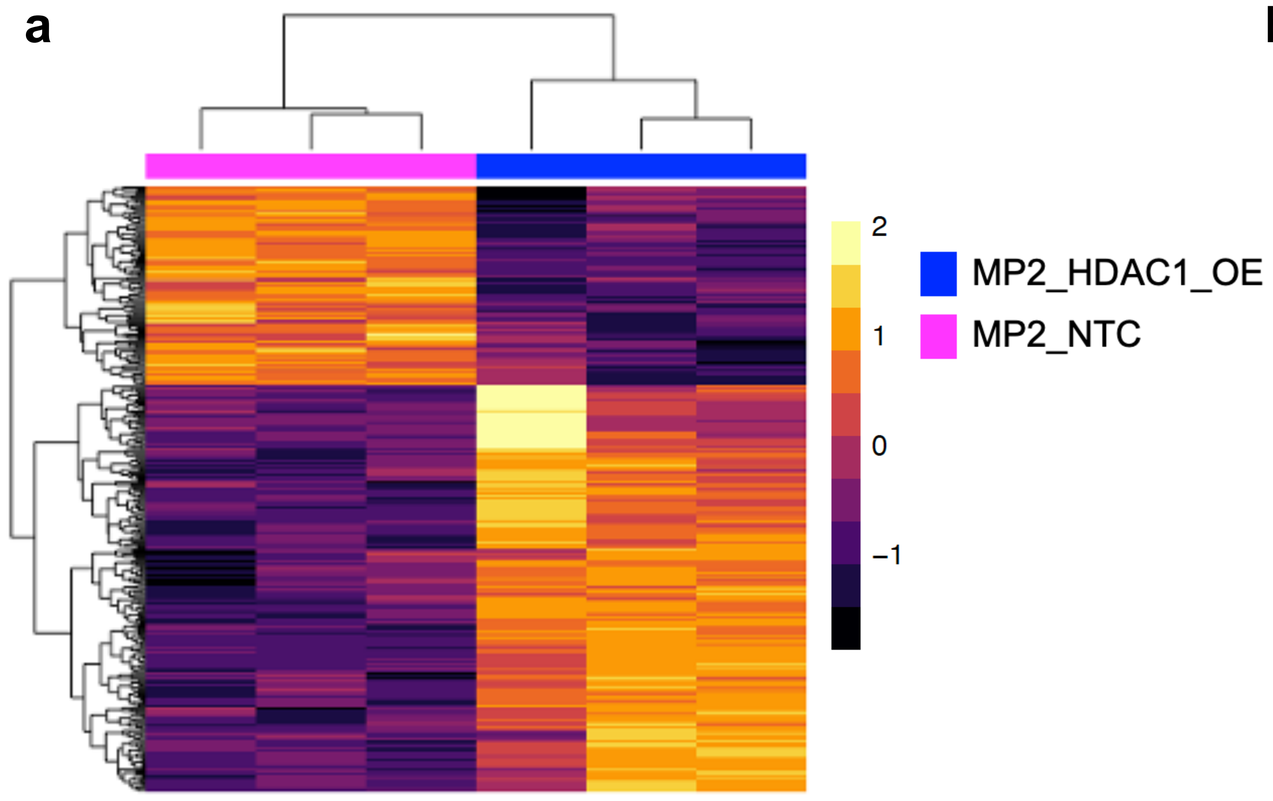
a
2
1
0
−1
MP2_HDAC1_OE
MP2_NTC

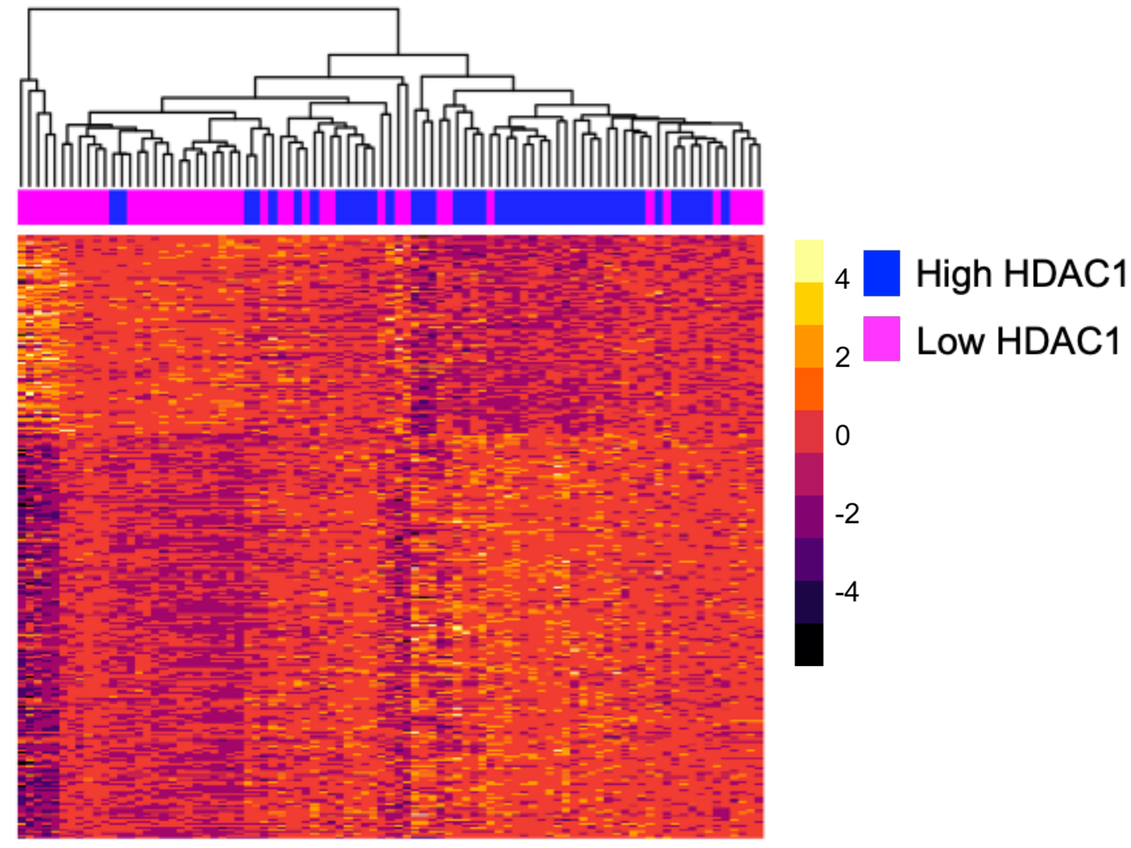
b
4
2
0
-2
-4
High HDAC1
Low HDAC1

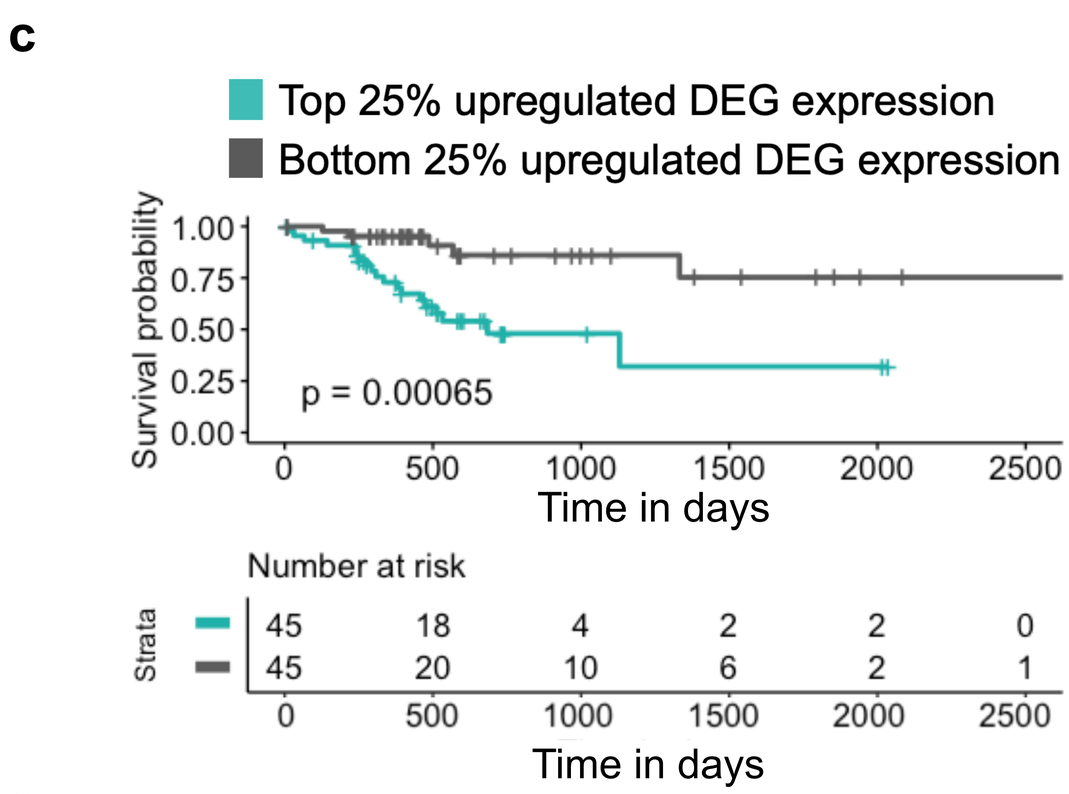
c
Top 25% upregulated DEG expression
Bottom 25% upregulated DEG expression
Survival probability
1.00
0.75
0.50
0.25
0.00
p = 0.00065
0
500
1000
1500
2000
2500
Time in days
Number at risk
Strata
45 18 4 2 2 0
45 20 10 6 2 1
Time in days

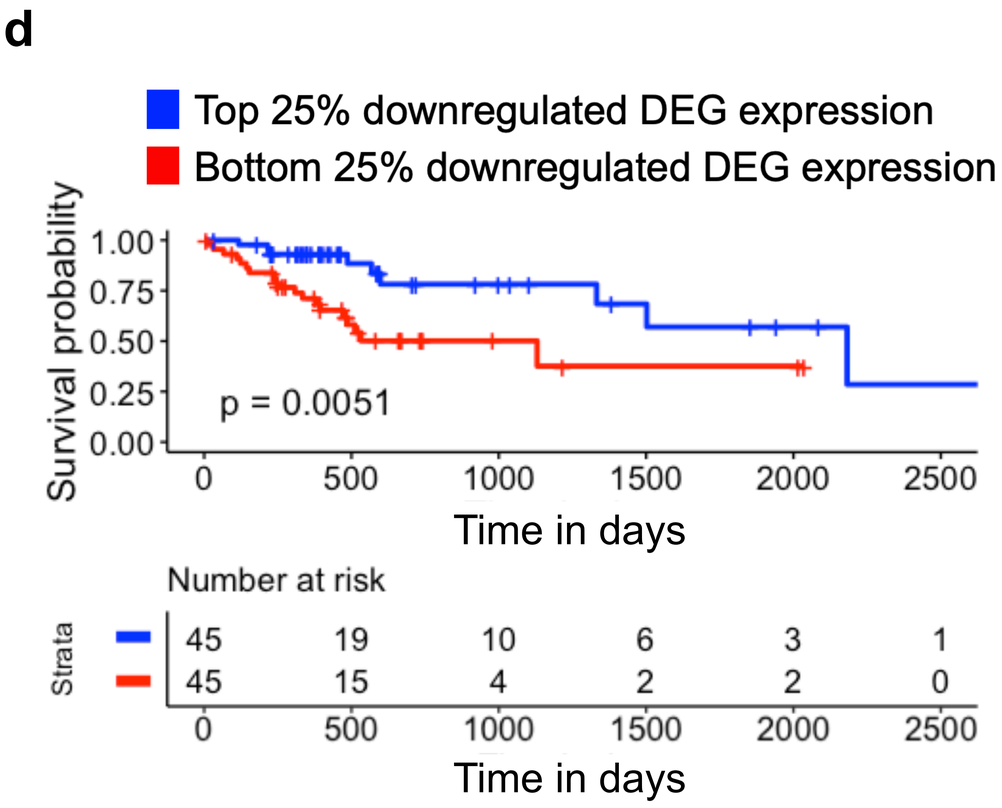
d
Top 25% downregulated DEG expression
Bottom 25% downregulated DEG expression
Survival probability
1.00
0.75
0.50
0.25
0.00
p = 0.0051
0
500
1000
1500
2000
2500
Time in days
Number at risk
Strata
45 19 10 6 3 1
45 15 4 2 2 0
Time in days

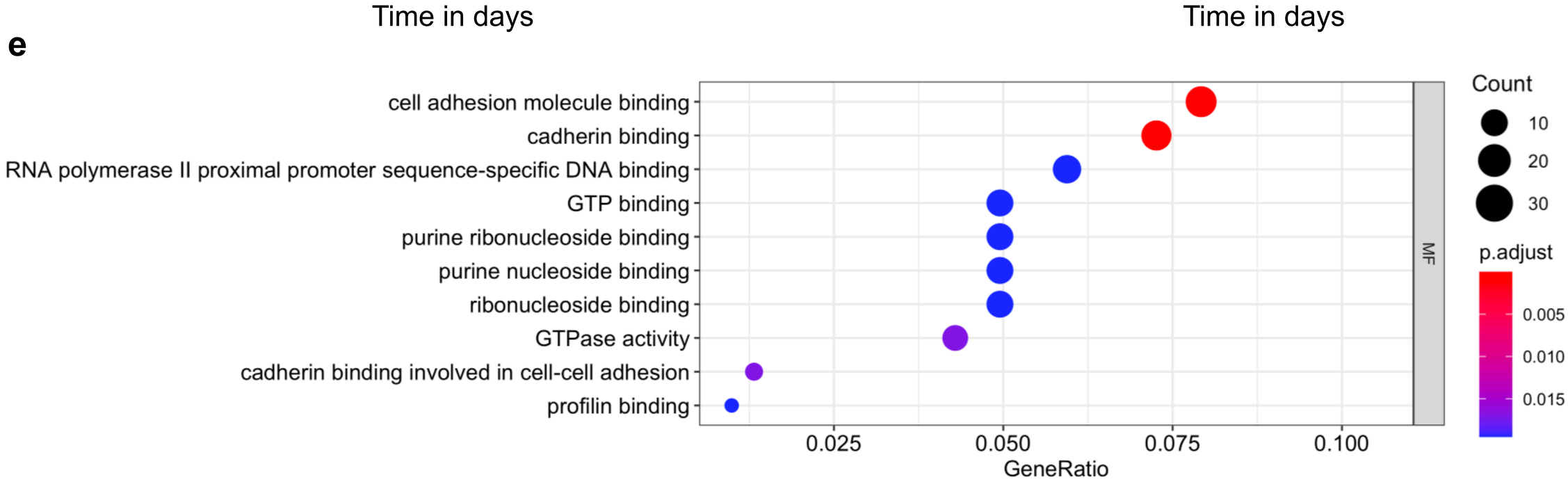
e
cell adhesion molecule binding
cadherin binding
RNA polymerase II proximal promoter sequence-specific DNA binding
GTP binding
purine ribonucleoside binding
purine nucleoside binding
ribonucleoside binding
GTPase activity
cadherin binding involved in cell-cell adhesion
profilin binding
MF
0.025
0.050
0.075
0.100
GeneRatio
Count
10
20
30
p.adjust
0.005
0.010
0.015

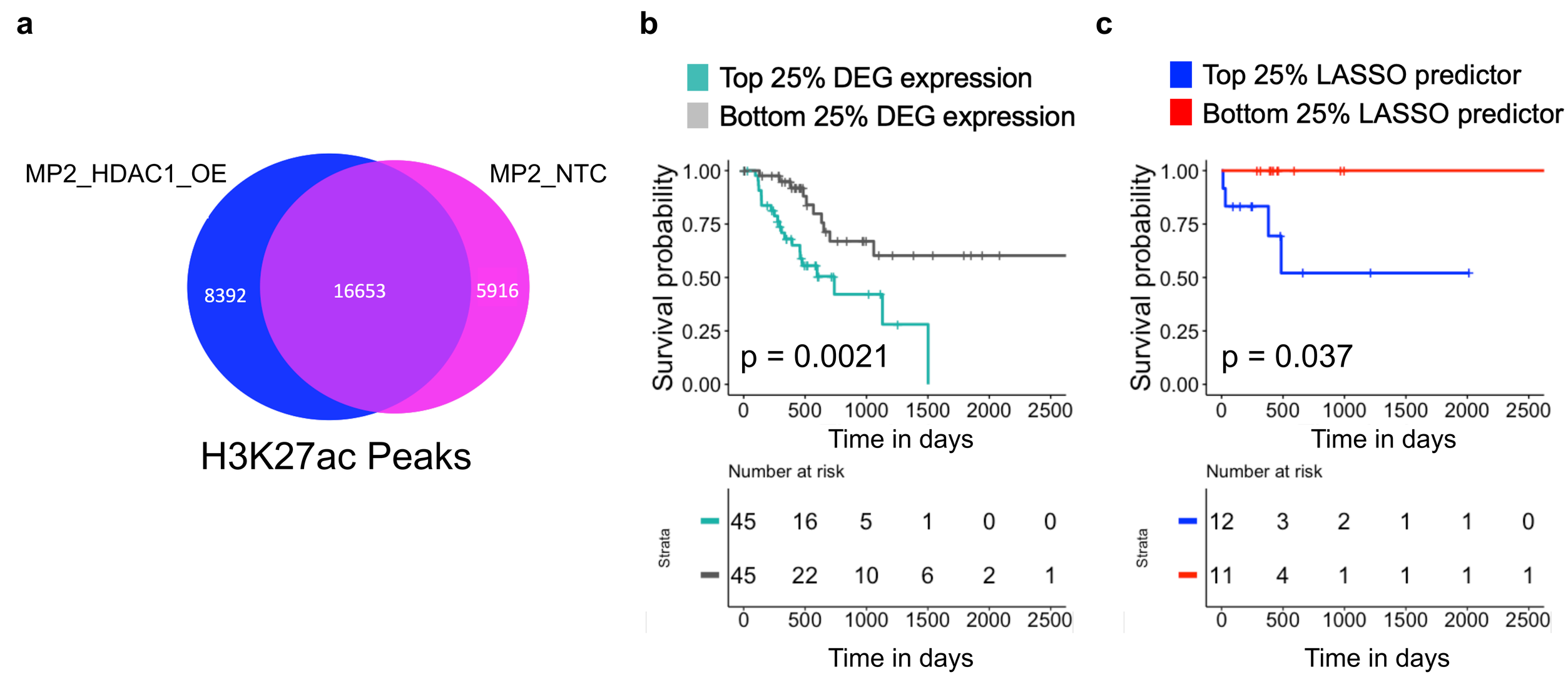
a
MP2_HDAC1_OE
MP2_NTC
8392
16653
5916
H3K27ac Peaks
b
Top 25% DEG expression
Bottom 25% DEG expression
Survival probability
1.00
0.75
0.50
0.25
0.00
p = 0.0021
0
500
1000
1500
2000
2500
Time in days
Number at risk
Strata
45 16 5 1 0 0
45 22 10 6 2 1
Time in days
c
Top 25% LASSO predictor
Bottom 25% LASSO predictor
Survival probability
1.00
0.75
0.50
0.25
0.00
p = 0.037
0
500
1000
1500
2000
2500
Time in days
Number at risk
Strata
12 3 2 1 1 0
11 4 1 1 1 1
Time in days

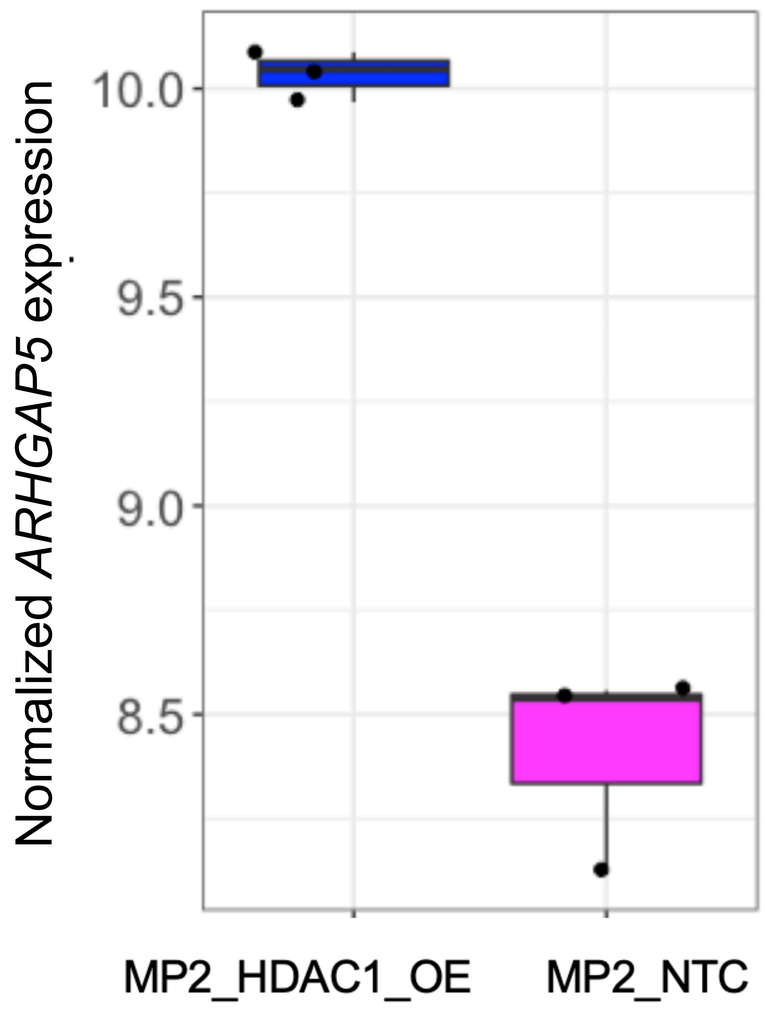
a
Normalized ARHGAP5 expression
10.0
9.5
9.0
8.5
MP2_HDAC1_OE
MP2_NTC

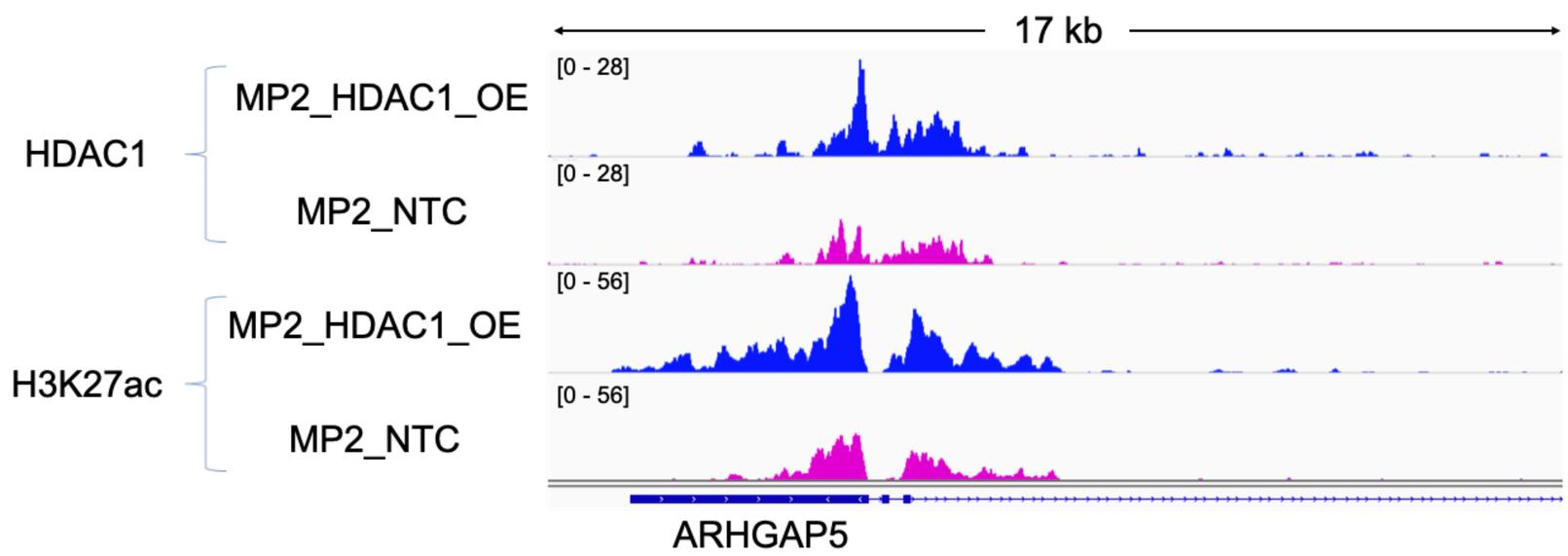
b
17 kb
HDAC1
MP2_HDAC1_OE
MP2_NTC
H3K27ac
MP2_HDAC1_OE
MP2_NTC
[0 - 28]
[0 - 28]
[0 - 56]
[0 - 56]
ARHGAP5

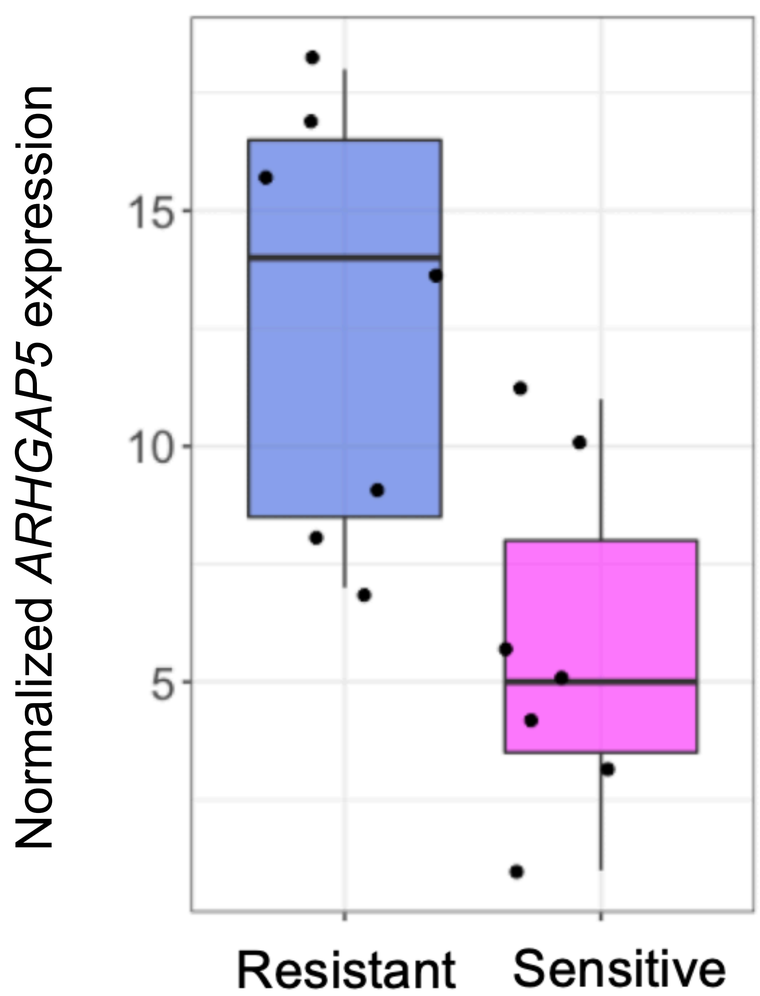
c
Normalized ARHGAP5 expression
15
10
5
Resistant
Sensitive

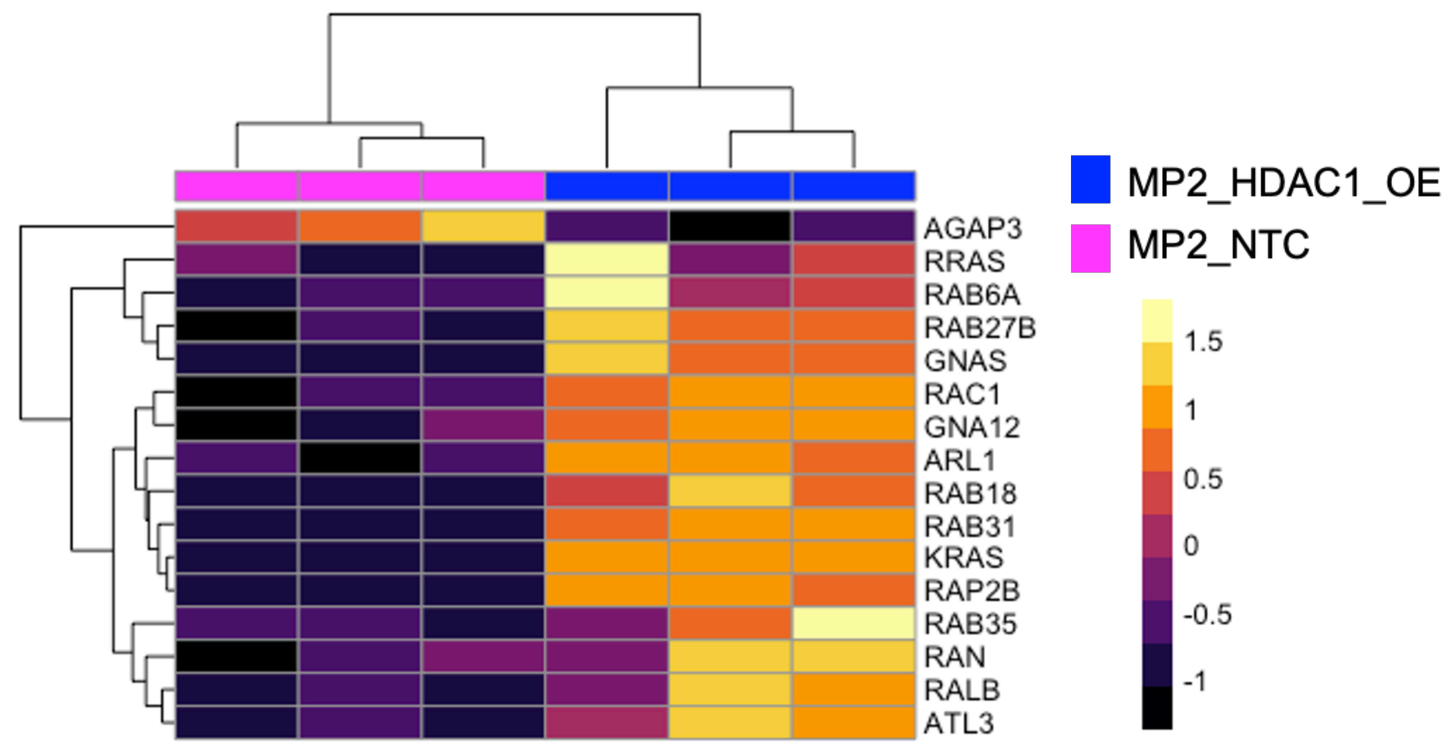
d
AGAP3
RRAS
RAB6A
RAB27B
GNAS
RAC1
GNA12
ARL1
RAB18
RAB31
KRAS
RAP2B
RAB35
RAN
RALB
ATL3
MP2_HDAC1_OE
MP2_NTC
1.5
1
0.5
0
-0.5
-1

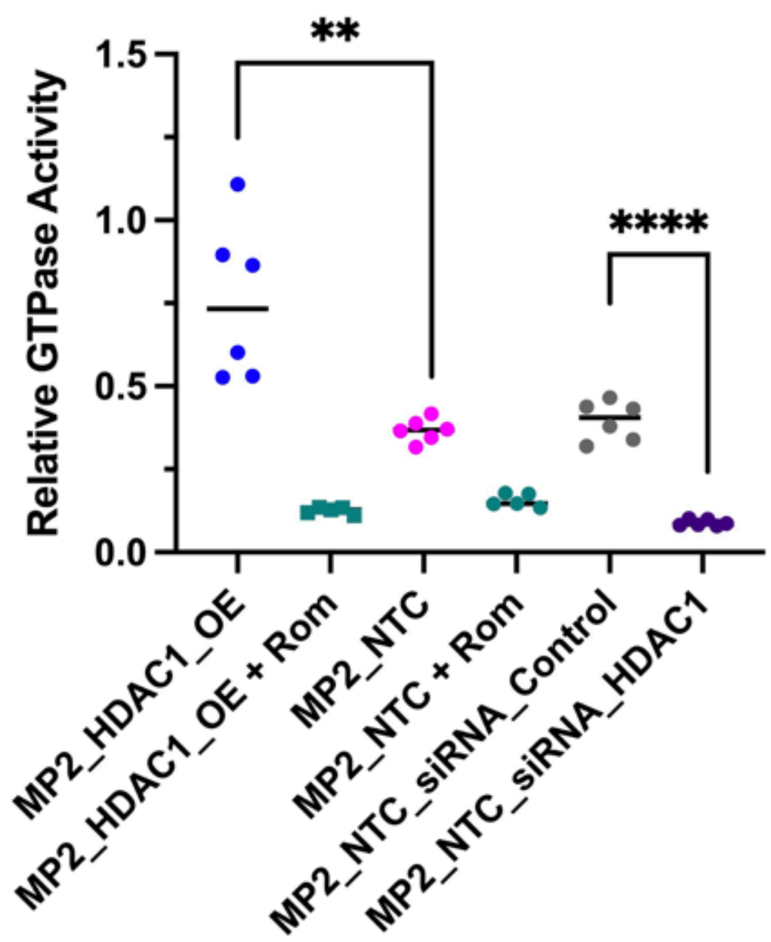
e
Relative GTPase Activity
1.5
1.0
0.5
0.0
**
****
MP2_HDAC1_OE
MP2_HDAC1_OE + Rom
MP2_NTC
MP2_NTC + Rom
MP2_NTC_siRNA_Control
MP2_NTC_siRNA_HDAC1